J|A|C|S
ARTICLES
Published on Web 04/19/2005

Ultrafast Energy-Electron Transfer Cascade in a Multichromophoric Light-Harvesting Molecular Square

Armin Sautter,[†] Başak Kükrer Kaletaş,[‡] Dietmar G. Schmid,[§] Rainer Dobrawa,[†] Mikhail Zimine,[‡] Günther Jung,[§] Ivo H. M. van Stokkum,[||] Luisa De Cola,[‡] René M. Williams,*[,‡] and Frank Würthner*[,†]

Contribution from the Institut für Organische Chemie, Universität Würzburg, Am Hubland, D-97074 Würzburg, Germany, Molecular Photonic Materials, van't Hoff Institute for Molecular Sciences, Universiteit van Amsterdam, Nieuwe Achtergracht 166, 1018 WV Amsterdam, The Netherlands, Institut für Organische Chemie, Universität Tübingen, Auf der Morgenstelle 18, D-72076 Tübingen, Germany, and Department of Physics and Astronomy, Vrije Universiteit, de Boelelaan 1081, 1081 HV Amsterdam, The Netherlands

Received August 27, 2004; E-mail: wuerthner@chemie.uni-wuerzburg.de; williams@science.uva.nl

Abstract: A molecular square with dimensions of about 4 nm, incorporating sixteen pyrene chromophores attached to four ditopic bay-functionalized perylene bisimide chromophores, has been synthesized by coordination to four Pt(II) phosphine corner units and fully characterized via NMR spectroscopy and ESI-FTICR mass spectrometry. Steady-state and time-resolved emission as well as femtosecond transient absorption studies reveal the presence of a highly efficient (>90%) and fast photoinduced energy transfer ($k_{en} \approx 5.0 \times 10^9$ s^{-1}) from the pyrene to the perylene bisimide chromophores and a very fast and efficient electron transfer (>94%, $k_{et} \approx 5 \times 10^{11}$ up to 43×10^{11} s^{-1}). Spectrotemporal parametrization indicates upper excited-state electron-transfer processes, various energy and electron-transfer pathways, and chromophoric heterogeneity. Temperature-dependent time-resolved emission spectroscopy has shown that the acceptor emission lifetime increases with decreasing temperature from which an electron-transfer barrier is obtained. The extremely fast electron-transfer processes (substantially faster and more efficient than in the free ligand) that are normally only observed in solid materials, together with the closely packed structure of 20 chromophoric units, indicate that we can consider the molecular square as a monodisperse nanoaggregate: a molecularly defined ensemble of chromophores that partly behaves like a solid material.

Introduction

Self-assembly of organic ligands with transition metal ions is a powerful method for the construction of supramolecular architectures. Molecular triangles, squares, catenanes, nano- and polytubes, and cages have been prepared as recently described in several excellent reviews.[1,2] The focus of current research in metallosupramolecular chemistry moves toward the introduction of functionality[3] into these systems such as redox activity,[4−6] magnetic[7] or luminescent properties,[4,8,9] and applications in the fields of molecular recognition,[9,10] sensing,[6,9] catalysis,[11] and electrochemical or photochemical switches.[12]

The metal−ligand interactions are stronger than other noncovalent bonds and are highly directional. As one of the most prominent examples, Pt(II) and Pd(II) complexes have been widely used to construct tetracoordinated square-planar species with 90° bond angles around the metal center capable of a perfect *cis* geometry. Especially for dpppPd(OTf)$_2$ and dpppPt(OTf)$_2$, numerous self-assembly processes with linear ditopic ligands afforded metallosupramolecular squares in quantitative yield under thermodynamic control.[2e,3a,13] On the basis of recent investigations by fluorescence and microcalorimetric methods,

[†] Universität Würzburg.
[‡] Universiteit van Amsterdam.
[§] Universität Tübingen.
[||] Vrije Universiteit.

(1) General reviews on self-assembly: (a) Prins, L. J.; Reinhoudt, D. N.; Timmerman, P. *Angew. Chem., Int. Ed.* **2001**, *40*, 2382−2426. (b) MacGillivray, L. R.; Atwood, J. L. *Angew. Chem., Int. Ed.* **1999**, *38*, 1018−1033. (c) Rebek, J. *Acc. Chem. Res.* **1999**, *32*, 278−286. (d) Philp, D.; Stoddart, J. F. *Angew. Chem., Int. Ed. Engl.* **1996**, *35*, 1154−1196. (e) Lawrence, D. S.; Jiang, T.; Levett, M. *Chem. Rev.* **1995**, *95*, 2229−2260.

(2) Reviews with focus on metallosupramolecular assemblies: (a) Holliday, B. J.; Mirkin, C. A. *Angew. Chem., Int. Ed.* **2001**, *40*, 2022−2043. (b) Leininger, S.; Olenyuk, B.; Stang, P. J. *Chem. Rev.* **2000**, *100*, 853−908. (c) Swiegers, G. F.; Malafetse, T. J. *Chem. Rev.* **2000**, *100*, 3483−3537. (d) Fujita, M. *Chem. Soc. Rev.* **1998**, *27*, 417−425. (e) Stang, P. J.; Olenyuk, B. *Acc. Chem. Res.* **1997**, *30*, 502−518. (f) Sun, W.-Y.; Yoshizawa, M.; Kusukawa, T.; Fujita, M. *Curr. Opin. Chem. Biol.* **2002**, *6*, 757−764.

(3) (a) Würthner, F.; You, C. C.; Saha-Möller, C. R. *Chem. Soc. Rev.* **2004**, *33*, 133−146. (b) Slone, R. V.; Benkstein, K. D.; Bélanger, S.; Hupp, J. T.; Guzei, I. A.; Rheingold, A. L. *Coord. Chem. Rev.* **1998**, *171*, 221−243.

(4) (a) Slone, R. V.; Hupp, J. T.; Stern, C.; Albrecht-Schmitt, T. E. *Inorg. Chem.* **1996**, *35*, 4096−4097. (b) Sun, S.-S.; Silva, A. S.; Brinn, I. M.; Lees, A. J. *Inorg. Chem.* **2000**, *39*, 1344−1345. (c) Sun, S.-S.; Lees, A. J. *Inorg. Chem.* **2001**, *40*, 3154−3160.

(5) (a) Funatsu, K.; Imamura, T.; Ichimura, A.; Sasaki, Y. *Inorg. Chem.* **1998**, *37*, 1798−1804. (b) You, C.-C.; Würthner, F. *J. Am. Chem. Soc.* **2003**, *125*, 9716−9725.

(6) (a) Lahav, M.; Gabai, R.; Shipway, A. N.; Willner, I. *Chem. Commun.* **1999**, 1937−1938. (b) Dinolfo, P. H.; Hupp, J. T. *Chem. Mater.* **2001**, *13*, 3113−3125 and references therein.

Scheme 1. Structures of the Pt(II) Assembled Molecular Squares Containing Four Perylene Units and 16 Pyrene Units (**Sq1**) or 16 *tert*-Butylphenoxy Units (**Sq2**) (Also Shown Are the Ligands **L1** and **L2**)

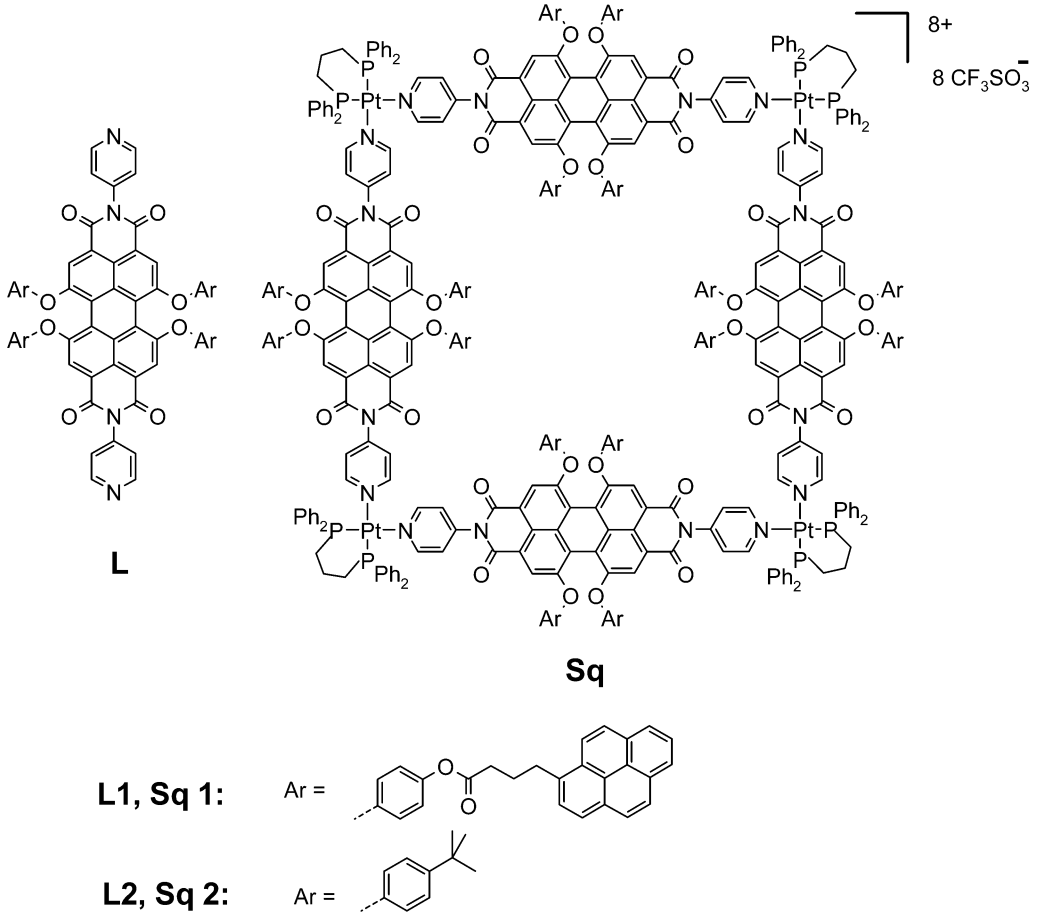

it could be established that these square assemblies remain intact at concentrations as low as $\sim 10^{-6}$ M in noncoordinating solvents such as dichloromethane and chloroform at room temperature.[3a,14] Therefore, in contrast to many hydrogen-bonded supramolecular architectures, these metallosupramolecular assemblies can be studied under dilute conditions, a prerequisite for steady-state and time-resolved emission spectroscopy.

The first metallosupramolecular squares that incorporate dyes have been synthesized by Drain and Lehn, as well as Stang, Hupp, and co-workers.[13b,15,16] In all of these cases, porphyrin dyes were applied, which, however, afforded only weakly luminescent assemblies. In more recent work, our group constructed molecular squares based on four perylene bisimide dyes. These squares exhibit superb fluorescence (quantum yield of ~90%) and electroactivity (multiple reverse reduction and oxidation waves in cyclic voltammetry).[8] Such square structures open up a promising avenue toward artificial light-harvesting systems, especially if we consider that the most developed natural light-harvesting systems all exhibit circular topology. However, the natural light-harvesting systems incorporate different types of dyes and contain much larger numbers of dyes within the self-assembled architecture. For example, crystallographically characterized bacterial light-harvesting assemblies LH II of *Rhodospirillum molischianum* are composed of 24 chlorophyll and 8 carotene dyes.[17]

Therefore, we initiated a program to develop molecular squares containing different types and larger numbers of chromophores and to study their photophysical properties. In this respect, energy and electron transfer from peripheral to central chromophores are the most desired functionalities as they form one of the keystones of natural photosynthesis. It is

(7) (a) Long, J. R. In *Chemistry of Nanostructured Materials*; Yang, P., Ed.; World Scientific Publishing: Hong Kong, 2003; pp 291−315. (b) Sokol, J. J.; Hee, A. G.; Long, J. R. *J. Am. Chem. Soc.* **2002**, *124*, 7656−7657. (c) Campos-Fernandez, C. S.; Clerac, R.; Dunbar, K. R. *Angew. Chem., Int. Ed.* **1999**, *38*, 3477−3479.
(8) (a) Würthner, F.; Sautter, A. *Chem. Commun.* **2000**, 445−446. (b) Würthner, F.; Sautter, A.; Schmid, D.; Weber, P. J. A. *Chem.-Eur. J.* **2001**, *7*, 894−902.
(9) Lee, S. J.; Lin, W. *J. Am. Chem. Soc.* **2002**, *124*, 4554−4555.
(10) (a) Whitford, J. A.; Stang, P. J.; Huang, S. D. *Inorg. Chem.* **1998**, *37*, 5595−5601. (b) Chang, S.-Y.; Jang, H.-Y.; Jeong, K.-S. *Chem.-Eur. J.* **2003**, *9*, 1535−1541. (c) Piotrowski, H.; Polborn, K.; Hilt, G.; Severin, K. *J. Am. Chem. Soc.* **2001**, *123*, 2699−2700. (d) Lehaire, M.-L.; Scopelliti, R.; Piotrowski, H.; Severin, K. *Angew. Chem., Int. Ed.* **2002**, *125*, 13683. (e) Ziegler, M.; Miranda, J. J.; Andersen, U. N.; Johnson, D. W.; Leary, J. A.; Raymond, K. *Angew. Chem., Int. Ed.* **2001**, *40*, 733−736.
(11) Merlau, M. L.; Mejia, M. P.; Nguyen, S. T.; Hupp, J. T. *Angew. Chem., Int. Ed.* **2001**, *40*, 4239−4242.
(12) (a) Chichak, K.; Branda, N. R. *Chem. Commun.* **1999**, 523−524. (b) Campbell, K.; McDonald, R.; Branda, N. R.; Tywinski, R. R. *Org. Lett.* **2001**, *3*, 1045−1048. (c) Sun, S.-S.; Anspach, J. A.; Lees, A. J. *Inorg. Chem.* **2002**, *41*, 1862−1869. (d) Schalley, C. A.; Müller, T.; Linnartz, P.; Witt, M.; Schäfer, M.; Lützen, A. *Chem.-Eur. J.* **2002**, *8*, 3538−3551.
(13) (a) Stang, P. J.; Cao, D. H. *J. Am. Chem. Soc.* **1994**, *116*, 4981−4982. (b) Fan, J.; Whiteford, J. A.; Olenyuk, B.; Levin, M. D.; Stang, P. J.; Fleischer, E. B. *J. Am. Chem. Soc.* **1999**, *121*, 2741−2752.
(14) Sautter, A.; Schmid, D. G.; Jung, G.; Würthner, F. *J. Am. Chem. Soc.* **2001**, *123*, 5424−5430.
(15) Drain, C. M.; Lehn, J.-M. *Chem. Commun.* **1994**, 2313−2315.
(16) Slone, R. V.; Hupp, J. T. *Inorg. Chem.* **1997**, *36*, 5422−5423.
(17) Hu, X.; Damjanovic, A.; Ritz, T.; Schulten, K. *Proc. Natl. Acad. Sci. U.S.A.* **1998**, *95*, 5935−5941. For another purple bacterial light-harvesting assembly (*Rhodopseudomonas acidophila*), 27 chlorophyll and 9 carotene dyes are arranged in a cyclic fashion, see: McDermott, G.; Prince, S. M.; Freer, A. A.; Hawthornthwaite-Lawless, A. M.; Papiz, M. Z.; Cogdell, R. J.; Isaacs, N. W. *Nature* **1995**, *374*, 517−521.

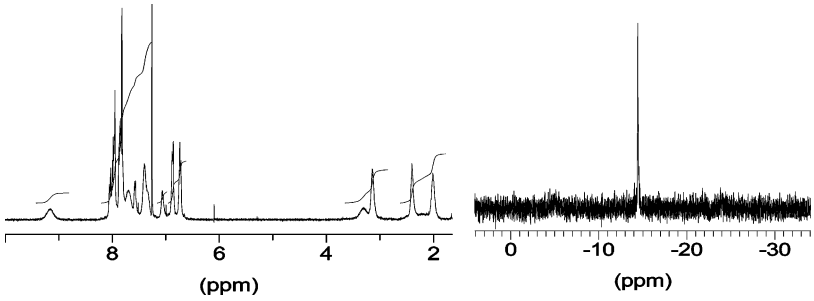

Figure 1. ^{1}H (left) and $^{31}P\{1H\}$ (right) NMR spectra of molecular square **Sq1** in $CDCl_3$.

important at this point to refer to related studies on light-harvesting dendrimers for which already pretty large structures containing many chromophores have been realized.[18,19]

In this paper, we describe the synthesis and investigate the photophysical properties of a Pt(II) ion assembled molecular square **Sq1** containing 16 pyrene chromophores tethered to the perylene bisimide square scaffold[20] and compare its properties to those of the related square without pyrene dyes (**Sq2**)[8] as well as their individual ligands (**L1** with four pyrene and **L2** with four *tert*-butylphenoxy units attached to the perylene bisimide moiety; see Scheme 1). The photoinduced processes of the pyrene-functionalized perylene bisimide **L1** have been reported recently.[21]

A quantitative analysis of the photophysical processes as well as their rates have been obtained by using UV−vis absorption, steady-state and time-resolved emission, femtosecond transient absorption spectroscopy, spectrotemporal analysis of the femtosecond transient absorption data, temperature-dependent time-resolved emission spectroscopy, and a theoretical analysis of the energetics of the processes. It has been found that efficient energy and electron-transfer processes occur from the pyrene chromophores to the perylene bisimide moieties in these photoactive molecular squares.

Results and Discussion

Synthesis and Structural Characterization. Equimolar mixing of ligand **L1** with [Pt(dppp)][$(OTf)_2$] in dichloromethane at room temperature leads to the formation of molecular square **Sq1** that could be precipitated by the addition of diethyl ether. NMR experiments (^{1}H and $^{31}P\{^{1}H\}$) indicate that the square forms quantitatively. However, due to an extremely fine precipitate, the isolated yield was only 67%.

The structure of **Sq1** was confirmed by ^{1}H and $^{31}P\{^{1}H\}$ NMR spectroscopy in $CDCl_3$, CD_2Cl_2, and CD_3NO_2 and ESI-FTICR-MS of dichloromethane/acetone solutions. The $^{31}P\{^{1}H\}$ NMR spectrum in $CDCl_3$ displays only one singlet at $\delta = -14.4$ ppm, shifted by about $\Delta\delta = 10$ ppm with respect to the precursor complex [Pt(dppp)][$(OTf)_2$], which is in accordance with the high symmetry of the square structure (Figure 1, right). In the ^{1}H NMR spectrum, typical changes of the pyridine H-protons ($\Delta\delta = 0.4$ ppm) are observed, and only one set of signals for the perylene bisimide ligand and one set for the dppp moiety are present (Figure 1, left).

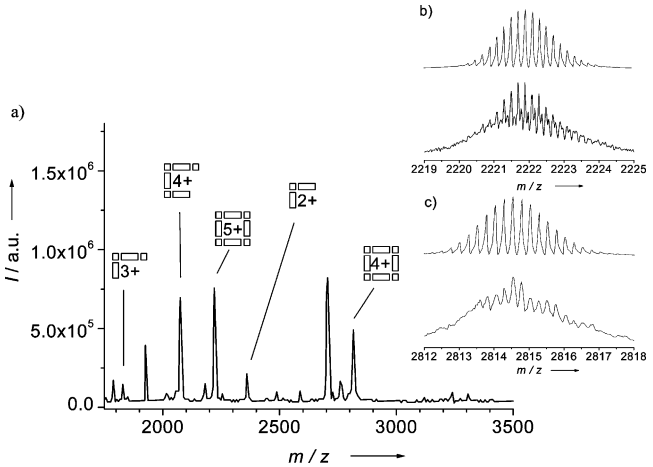

Figure 2. (a) ESI-FTICR-MS of **Sq1** (solution in acetone/CH_2Cl_2, 1:1); (b,c) comparison of the calculated (top) and measured (bottom) spectra of the (b) [**Sq1**−5OTf]$^{5+}$ and (c) [**Sq1**−4OTf]$^{4+}$ species.

Most signals are significantly broadened, which indicates restricted conformational flexibility as already found and discussed for related squares.[5,8,13] In the ^{1}H NMR spectrum of **Sq1**, the methylene groups of the propyl bridges that tether the pyrenes to the perylene bisimide are also broad and unstructured. If rotation of the perylene bisimide moiety within the square scaffold is normally thought to occur rapidly on the NMR time scale, this rotation might slow considerably for **Sq1** due to the sterical demand of the pyrenes.

ESI-FTICR-MS provided unambiguous evidence for tetrameric assemblies and their stability even in the gas phase. The overview spectrum of **Sq1** displays the intact square species [**Sq1**−4OTf]$^{4+}$ at *m*/*z* 2814.54 and [**Sq1**−5OTf]$^{5+}$ at *m*/*z* 2221.87 after the loss of four and five triflate anions, respectively (Figure 2). Deconvolution of the two signals amounts to a molecular mass of 11 854.40 and 11 854.65 Da, respectively, which is in excellent agreement with the calculated average mass of 11 855.65 Da. Several fragments could also be identified, for example, loss of one corner (C) and one diaza ligand (L) [**Sq1**−1C−1L]$^{4+}$, *m*/*z* 2073.77; loss of two corners and two

(18) For light-harvesting dendrimers incorporating perylene imide dyes, see: (a) Weil, T.; Wiesler, U. M.; Herrmann, A.; Bauer, R.; Hofkens, J.; De Schryver, F. C.; Müllen, K. *J. Am. Chem. Soc.* **2001**, *123*, 8101−8108. (b) Weil, T.; Reuther, E.; Müllen, K. *Angew. Chem., Int. Ed.* **2002**, *41*, 1900−1904. (c) Serin, J. M.; Brousmiche, D. W.; Fréchet, J. M. J. *Chem. Commun.* **2002**, 2605−2607. (d) Serin, J. M.; Brousmiche, D. W.; Fréchet, J. M. J. *J. Am. Chem. Soc.* **2002**, *124*, 11848−11849. (e) Gronheid, R.; Stefan, A.; Cotlet, M.; Hofkens, J.; Qu, J.; Müllen, K.; Van der Auweraer, M.; Verhoeven, J. W.; De Schryver, F. C. *Angew. Chem., Int. Ed.* **2003**, *42*, 4209−4214. (f) Ahrens, M. J.; Sinks, L. E.; Rybtchinski, B.; Liu, W.; Jones, B. A.; Giaimo, J. M.; Gusev, A. V.; Goshe, A. J.; Tiede, D. M.; Wasielewski, M. R. *J. Am. Chem. Soc.* **2004**, *126*, 8284−8294.

(19) For a recent review on photoinduced processes in dendrimers, see: (a) Dirksen, A.; De Cola, L. *C. R. Chimie* **2003**, *6*, 873−882. See also: (b) *Dendritic Molecules: Concepts, Syntheses, Perspectives*; Newkome, G. R., Moorefield, C. N., Vögtle, F., Eds.; VCH: New York, 1996. (c) *Top. Curr. Chem.*; Vögtle, F., Ed.; Wiley−Interscience: New York, Vol. 197 (1998), Vol. 210 (2001), Vol. 217 (2002).

(20) Part of this work was published as a communication: Würthner, F.; Sautter, A. *Org. Biomol. Chem.* **2003**, *1*, 240−243.

(21) Kaletas Kükrer, B.; Dobrawa, R.; Sautter, A.; Würthner, F.; Zimine, M.; De Cola, L.; Williams, R. M. *J. Phys. Chem. A* **2004**, *108*, 1900−1909.

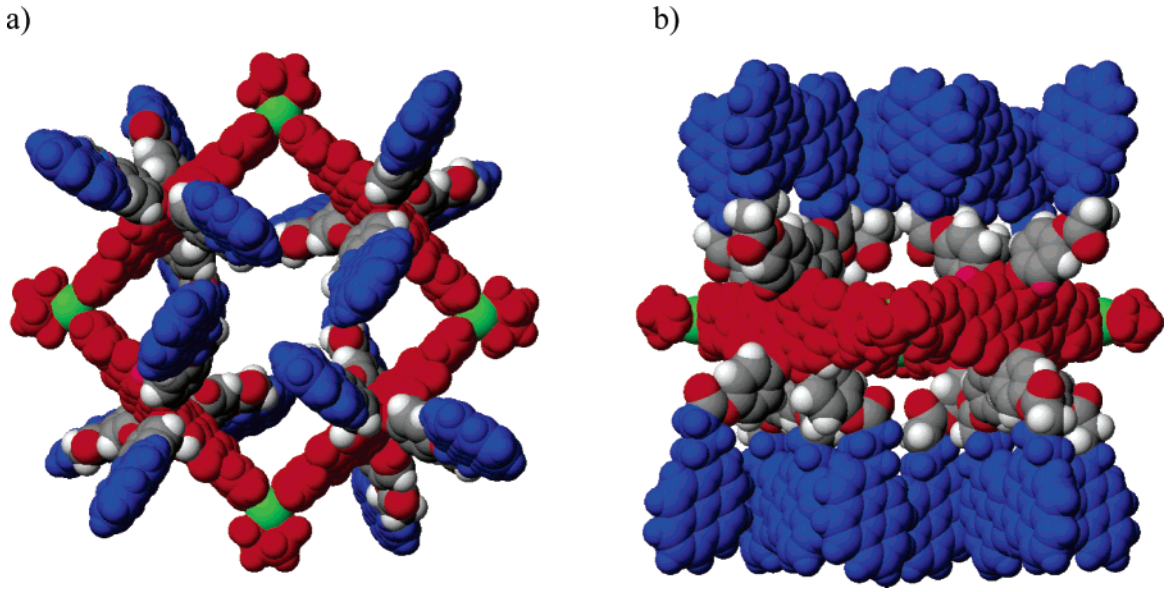

Figure 3. (a) Top and (b) side view of a MD-MM2 geometry optimization of light-harvesting molecular square **Sq1**. For simplicity and to reduce the number of atoms, the phosphane ligand was replaced by a simple ethylene diamino chelate ligand. Pyrenes, blue; perylene bisimides, red.

diaza ligands [**Sq1**−2C−2L]$^{3+}$, *m*/*z* 1826.80; and loss of three corners and two diaza ligands [**Sq1**−3C−2L]$^{2+}$, *m*/*z* 2361.63.

Because of the high molecular mass of 11 855.65 Da and the poor solubility of **Sq1** in acetone, the detection of the multiply charged intact square species was difficult, that is, ionization without encountering dissociation of the square. Therefore, the resolution of the signals is not as good as for some other squares, which we have characterized previously by this method.[8,14] Nevertheless, the direct comparison of the [**Sq1**−5OTf]$^{5+}$ at *m*/*z* 2221.87 and [**Sq1**−4OTf]$^{4+}$ at *m*/*z* 2814.54 species with the calculated spectra leaves no doubt about the results. The spectra are in good agreement with the calculated isotope pattern as is shown in Figure 2b,c, and thereby species of the same *m*/*z* ratio but of different charge states can be ruled out.

To get a better idea about the sterical situation and the most likely arrangement of the chromophores within molecular square **Sq1**, molecular modeling and molecular dynamics simulations (MD-MM2) were carried out. Because of the size, number of atoms, and complexity of the structure, it is impossible to find the global energy minimum, and the outcome of the optimization strongly depends on the starting geometry. Therefore, the energetically most favorable structure shown in Figure 3 should be regarded as a snapshot of one of the possible conformations of **Sq1** and rather give an impression of the relative size and bulkiness of the substituents. In particular, we like to emphasize that only the perylene bisimide square is fixed rigidly in space, while the pyrene chromophores exhibit conformational flexibility. Nevertheless, it is justified to distinguish between "inner" and "outer" pyrene dyes (Figure 3a) and those above and below the plane of the perylene bisimide square (Figure 3b).

Steady-State Spectroscopy. The optical properties of **Sq1**, **Sq2**, **L1**, and **L2** have been studied with UV−vis absorption and emission spectroscopy. The UV−vis absorption spectra of **L1**, **L2**, and **Sq1** in dichloromethane are depicted in Figure 4, and the photophysical data are summarized in Table 1. The ground-state properties of the squares are very similar to those of the components because the complexation with Pt(II) ion results in a very weak electronic coupling between the units. The pyrene absorption bands of **L1** and **Sq1** dominate the UV region of the spectrum with five sharp characteristic pyrene transitions (see Figure 4). The absorption bands of the perylene

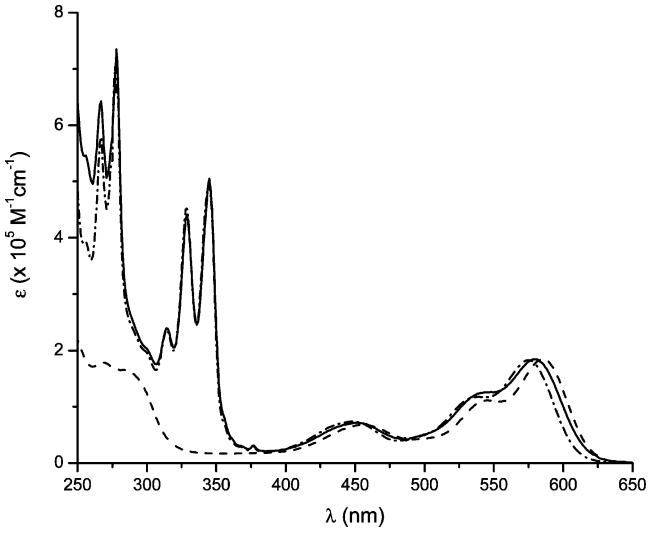

Figure 4. Comparison of the absorptions of **L1** (− · − · −), **L2** (− − −), and **Sq1** (−) in dichloromethane. For comparison, the extinction coefficients of **L1** and **L2** were multiplied by a factor of 4.

Table 1. Summary of the Photophysical Properties of **L1**, **L2**, **Sq1**, and **Sq2** in Dichloromethane at Room Temperature[a]

	emission					
cmpds	λ_{pyr} (nm)	λ_{per} (nm)	τ_{pyr} (ns)	τ_{per} (ns)[b]	Φ_{pyr}	Φ_{per}
L1	378	611	0.24	1	0.0011	0.12[c,d]
L2		620		8.5		0.88[e]
Sq1	377	619	0.23	0.93	0.0008	0.05[f]
Sq2		630		5.5		0.83[e]

[a] Excitation wavelength for lifetimes is 324 nm unless otherwise indicated. [b] The following main rise times were also observed only for the perylene emission: 0.21 ns for **L1** and 0.18 ns for **Sq1**. [c] λ_{ex} = 336 nm. [d] λ_{ex} = 545 nm. [e] λ_{ex} = 430 nm. [f] Both λ_{ex} = 307 nm and λ_{ex} = 550 nm, with respect to *N*,*N*′-di(2,6-diisopropylphenyl)-1,6,7,12-tetraphenoxyperylene-3,4:9,10-tetracarboxylic acid bisimide, by the measurement of front-face emission.

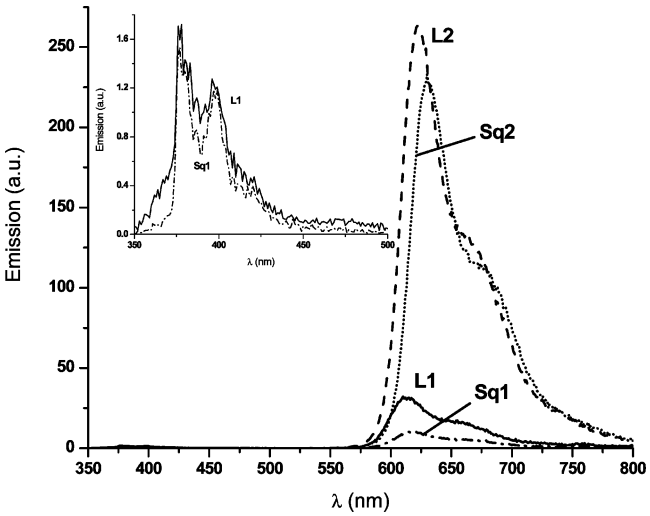

Figure 5. Front-face emission spectra of **L1** (−), **L2** (− − −), **Sq1** (− · − · −), and **Sq2** (· · · ·) in dichloromethane, $\lambda_{ex} = 336$ nm. Inset: Expansion of the pyrene emission region.

bisimide units with the characteristic $\pi-\pi^*$ transitions in the visible[22,23] are present in all compounds. Upon coordination of the platinum ion in the squares, **Sq1** and **Sq2** bathochromic shifts of 5 and 6 nm (150 and 174 cm^{-1}) are observed for the electronic transitions of the perylene bisimide units for **Sq1** and **Sq2** (as compared to the absorption spectra of the corresponding ligands). Such bathochromic shifts were observed before and attributed to the coordination of the pyridine receptor unit to the Pt(II) metal ion.[8] Another difference between the absorption spectra of the ligands and the squares is the weak shoulder observed for the latter between 250 and 280 nm, which might be caused by the metal moieties.[24−27] No distinct additional or new optical transitions in the visible region related to the metal phosphine corners or a MLCT band were observed for the squares.

As was previously studied in **L1**,[21] the distinct absorption patterns belonging to the 16 pyrene moieties in the UV region, and the four perylene units in the visible, allow a highly selective excitation of the individual pyrene and perylene bisimide chromophores in **Sq1**. It is interesting to note that the perylene bisimide absorption bands of **L1** and **Sq1** are ca. 10 nm higher in energy as compared to those of **L2** and **Sq2**, which appears to be due to the presence of the ester groups in the phenoxy substituents.

The front-face emission spectra[28] of all compounds (Figure 5) in dichloromethane at room temperature were recorded upon excitation at 336 nm. At this wavelength, the main absorption comes from the pyrene units present only in **L1** and **Sq1**. The pyrene moieties in **Sq1** emit very weakly between 380 and 460 nm as in the component **L1**.[21] This quenched emission could indicate either an energy transfer from the higher pyrene excited state to the lower perylene excited state or an electron-transfer process from the donor (pyrene) moiety to the perylene electron acceptor unit. Apart from the strongly quenched pyrene emission (vide infra), **Sq1** displays a weakly sensitized fluorescence from the lower lying excited state of the perylene chromophore (see Figure 5, − · − · −). All compounds show a typical perylene emission[29] with a maximum between 618 and 630 nm and a shoulder at 665−685 nm. For **L1** and **Sq1**, there is an 8 nm (212 cm^{-1}) difference in the perylene emission maximum, while this value is 10 nm (256 cm^{-1}) for **L2** and **Sq2**, that is, a slightly larger shift as observed in the absorption spectra. However, as compared to the systems **L2** and **Sq2**, which do not contain pyrene units, the emission intensities of the perylene units of **L1** and **Sq1** are strongly quenched. Especially for the self-assembled square **Sq1**, the quenching is much more pronounced than for its corresponding component **L1**.

No additional emission or absorption bands were observed due to either excimer and/or exciplex formation. The photophysical properties of all compounds are summarized in Table 1.

The emission quantum yields of **Sq1** and **L1** were determined for both the pyrene and the perylene emissions, by exciting in the UV and visible regions, as indicated in Table 1. In both **Sq1** and **L1**, the pyrene moiety is strongly quenched as compared to a reference compound, pyrene $\Phi_f = 0.65$, in nonpolar solvent.[30] As can be seen from Table 1, the assembly through the Pt(II) ions does not influence the emission of the pyrene moiety. In fact, almost the same pyrene quantum yields are observed for **L1** (0.0011) and **Sq1** (0.0008).

The perylene bisimide emission of the self-assembled pyrene-perylene bisimide square **Sq1** is clearly quenched as compared to the model compound **Sq2**. Even compared to the pyrene containing ligand **L1**,[21] the perylene bisimide emission is reduced to almost 40%. Regardless of the excitation wavelength, that is, excitation in both the UV and the visible region, the quantum yield of perylene emission for the **Sq1** is found to be 0.05.

The emission spectra and the data in Table 1 indicate that, apart from the energy transfer from excited pyrene to perylene bisimide chromophores, an additional process, electron transfer, takes place that quenches the perylene bisimide emission. This electron transfer is more efficient in the coordination compound **Sq1** than in the free ligand **L1**. A reasonable explanation is that the complexation of the Pt(II) ion on the pyridine receptor units connected to the perylene moieties results in a lowering of the LUMO (lowest unoccupied molecular orbital) energy of the perylene bisimide as has been demonstrated by a 70 mV shift of the redox potential for the perylene bisimide unit in **Sq2** as compared to **L2** by cyclic voltammetry.[8] Accordingly, quenching by electron transfer would be more exergonic.[31]

Time-Resolved Emission Spectroscopy. As was shown by steady-state spectroscopy, additional photophysical processes are occurring when pyrene units are attached to the perylene bisimide systems (**L1**, **Sq1**). To shed more light on these

(22) Gvishi, R.; Reisfeld, R.; Burshtein, Z. *Chem. Phys. Lett.* **1993**, *213*, 338−344.
(23) Liu, D.; De Feyter, S.; Cotlet, M.; Stefan, A.; Wiesler, U.-M.; Herrmann, A.; Grebel-Koehler, D.; Qu, J.; Müllen, K.; De Schryver, F. C. *Macromolecules* **2003**, *36*, 5918−5925.
(24) Balashev, K. P.; Puzyk, M. V.; Kotlyar, V. S.; Kulikova, M. V. *Coord. Chem. Rev.* **1997**, *159*, 109−120.
(25) Chen, Y.-H.; Merkert, J. W.; Murtaza, Z.; Woods, C.; Rillema, D. P. *Inorg. Chim. Acta* **1995**, *240*, 41−47.
(26) Lu, W.; Chan, M. C. W.; Cheung, K.-K.; Che, C.-C. *Organometallics* **2001**, *20*, 2477−2486.
(27) Wang, F.; Wu, X.; Finnen, D. C.; Neckers, D. C. *Tetrahedron Lett.* **2000**, *41*, 7613−7617.
(28) As self-assembled molecular squares dissociate into their constituent parts upon dilution, the concentration had to be kept at 10^{-6} M or higher. Due to the high optical density for the pyrene absorption region at this concentration, front-face emission measurements were performed.
(29) Zeiny, E.; Eldaly, S. A.; Langhals, H. *J. Phys. Chem.* **1988**, *92*, 4565−4568.
(30) Murov, S.; Carmichael, I.; Hug, G. L. *Handbook of Photochemistry*, 2nd ed.; Marcel Dekker: New York, 1993.

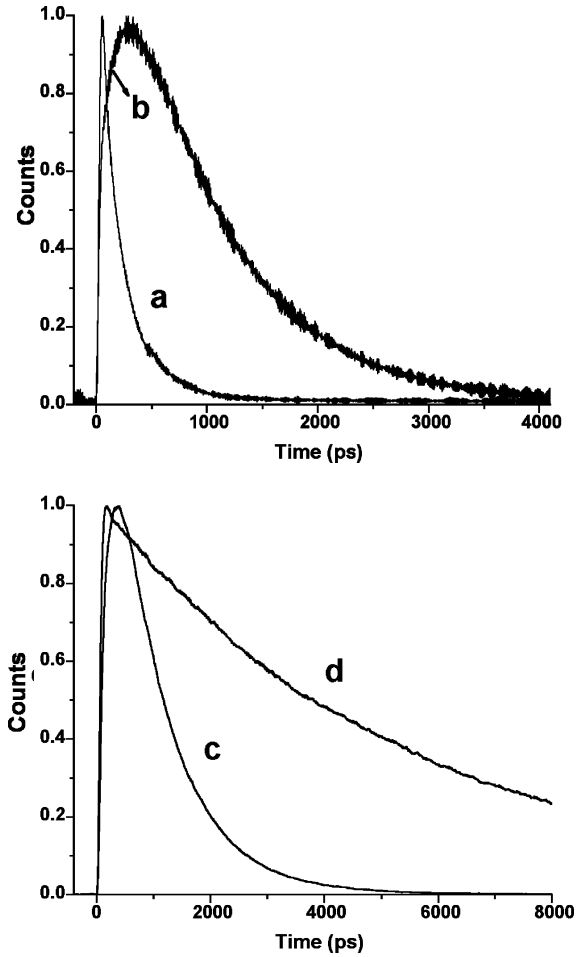

Figure 6. Time-resolved emission traces of **Sq1** and **Sq2** in dichloromethane at room temperature (measured with single photon counting, $\lambda_{ex} = 324$ nm). The quenched lifetime of the pyrene moiety of **Sq1** measured at 400 nm (a), the rise time of the perylene unit of **Sq1** at 615 nm (b). The quenched emission of the perylene unit of **Sq1** at 615 nm (c), emission of **Sq2** probed at 615 nm (d). All traces are deconvoluted signals.

processes, time-resolved emission by monitoring the perylene (all compounds) and the pyrene emission (for **Sq1** and **L1**) was performed. The time-resolved emission decays for **Sq1** and **Sq2** are depicted in Figure 6. Upon excitation of the pyrene unit, quenching of the pyrene excited state and the formation of the perylene excited state is observed in **Sq1** (see Figure 6, traces a and b). In Figure 6 (bottom), a comparison is made between the quenched emission of **Sq1** (trace c) and the highly emitting **Sq2** (trace d). The model square **Sq2** shows a monoexponential decay.

For **Sq1**, a sensitization of the emission of the perylene unit with a main rise time of 178 ps is observed. This is in good agreement with the main (75%) quenched pyrene excited-state lifetime (231 ps; a minor component (25%) of 23 ps is also observed) (see Figure 6). This suggests that energy transfer from the excited pyrene to the perylene moieties occurs. However, as already mentioned, the emission of the perylene unit is also quenched, and its excited-state lifetime is reduced from 5.5 ns (**Sq2**) to a major lifetime of 930 ps. According to these time-resolved emission results, the average rate of energy transfer can be calculated from the main rise time of the perylene and main decay value of the pyrene, mentioned above, using the following equation:

$$k_{en} = 1/\tau - 1/\tau_{ref} \quad (1)$$

where τ and τ_{ref} represent the excited-state lifetime of the pyrene moiety in the **Sq1** and the lifetime of the reference pyrene ($\tau_{ref} = 650$ ns),[30] respectively. The average rate constant for the energy-transfer process for **Sq1** thus results as $k_{en} = 5.0 \times 10^9\ s^{-1}$.

By using the experimentally obtained energy-transfer rate, the donor−acceptor distance (R) can be calculated (8−11 Å) employing the Förster theory, as reported for **L1**.[21]

It is interesting to notice that the rate is slightly faster than the reported value for the nonassembled component **L1** ($4.2 \times 10^9\ s^{-1}$). The difference could be attributed to the higher chromophore density in the assembly, which might enable additional energy-transfer pathways between pyrene and perylene bisimide units of different ligands. Furthermore, the presence of the metal ions at the corners of the square should confer to the assembled systems a higher rigidity and a lowering of the nonradiative processes in the supramolecular complex.

The short decay time (0.93 ns) and the low emission quantum yield (0.05) detected for the perylene bisimide units in **Sq1** as compared to the **Sq2** (see Table 1) indicate that an electron-transfer process takes place, quenching the emission of the perylene unit. Due to the short lifetime measured for the perylene-based component in **Sq1**, we have performed further investigations by femtosecond time-resolved transient spectroscopy.

Femtosecond Transient Absorption Spectroscopy. More detailed information about the excited-state properties of **Sq1** and **Sq2** has been acquired by using femtosecond transient absorption spectroscopy. The spectra of compounds **Sq1** and **Sq2** and single line kinetics belonging to **Sq1** in dichloromethane are depicted in Figures 7 and 8.

For the reference compound **Sq2**, almost identical transient absorption spectra are observed upon excitation at 345 and 575 nm. They show an intense bleaching around 625 nm and a strong $S_1 \rightarrow S_n$ perylene bisimide excited-state transition centered at 730 nm. No recovery of the ground state was observed within our instruments time frame because, as previously mentioned, the excited-state lifetime is in the nanosecond time regime.

In contrast, for compound **Sq1**, significant differences are observed. Upon UV excitation of the pyrene (345 nm), the following processes occur:

(a) The instantaneous development of maxima at 482 and 514 nm: These bands are typical for $S_1 \rightarrow S_n$ transitions of pyrene.[32]

(31) A similar effect on the quenching efficiency could be observed by replacing the "innocent" Pt(II) ion with a simple proton. Thus, TFA (trifluoroacetic acid) was added to a solution of **L1** in dichloromethane, and the changes in the absorption and emission spectra were detected. Upon addition of TFA, a bathochromic shift of 15 nm (442 cm^{-1}) was observed in absorption and a decrease in the emission intensity together with a shift of 22 nm (574 cm^{-1}) to longer wavelength was detected. Accordingly, protonation gives effects similar to metal ion complexation and results in an increased quenching of the perylene emission, indicating that also protonation at the pyridine units makes the perylene bisimide a better acceptor. Similar bathochromic shifts in the absorption spectra upon protonation of the chromophore *fac*-$Re(CO)_3Cl(4,4'\text{-bpy})_2$, where two units were coordinating with Pd(II) metal ions to form a molecular square, have been observed in the literature: (a) Slone, R. V.; Yoon, D. I.; Calhoun, R. M.; Hupp, J. T. *J. Am. Chem. Soc.* **1995**, *117*, 11813−11814. (b) Wrighton, M. S.; Giordano, P. J. *J. Am. Chem. Soc.* **1979**, *101*, 2888−2897.

(32) Foggi, P.; Pettini, L.; Righini, R.; Califano, S. *J. Phys. Chem.* **1995**, *99*, 7439−7445.

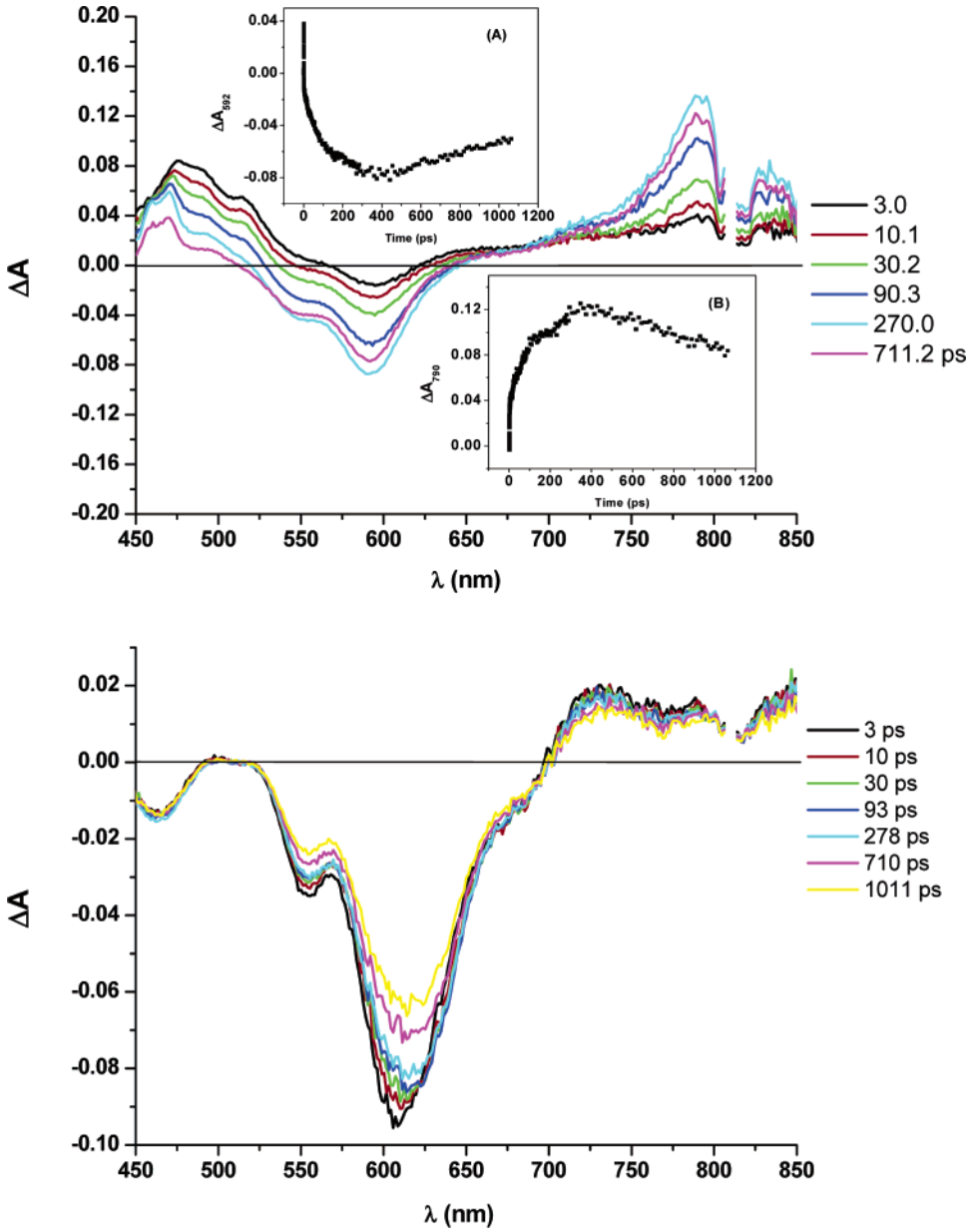

Figure 7. Femtosecond transient spectra of **Sq1** (top) and **Sq2** (bottom) in dichloromethane; time delays corresponding to frames are given in the spectra (λ_{ex} = 345 nm, 130 fs fwhm). Kinetic profile of the transient absorption measured (A) at 592 nm, (B) at 790 nm.

(b) Bleaching at 590 nm with a time constant of 120 ps (cp. Figure 7, inset A): This bleaching indicates the depopulation of the perylene bisimide ground state and, therefore, provides additional evidence for the pyrene to perylene energy transfer observed in emission spectroscopy.

(c) Formation of absorption bands at 470 nm (with a shoulder at 489 nm) and at 780 nm: The former bands can be attributed to the pyrene radical cations,[33] and the latter is indicative for perylene bisimide radical anions. Such bands, therefore, confirm that a fast electron transfer takes place from the pyrene (donor) to the perylene bisimide (acceptor) units. Analysis of the kinetics at 789 nm gives a rise time of 145 ps.

(d) The final process is the decay of the perylene bisimide radical anion band with a time constant of about 1.9 ns due to the back electron transfer (cp. Figure 7, inset B).

(33) Kawai, K.; Takada, T.; Tojo, S.; Ichinose, N.; Majima, T. *J. Am. Chem. Soc.* **2001**, *123*, 12688−12689.

For the direct excitation of the perylene bisimide dyes at 575 nm (Figure 8), the following changes are observed:

(a) formation of pyrene radical cations and perylene bisimide radical anions on a much faster time scale of about 2 ps, and

(b) back electron transfer on a time scale of about 1.2−1.8 ns.

It has to be realized that the longest time delay available with our setup is 1 ns, which accounts for the spread in the longer lifetimes.

The major difference observed in the femtosecond spectroscopy between the self-assembled square **Sq1** and the component **L1**[21] lies in the more intense absorption of the radical anion of the perylene bisimide moiety, independent of the excitation wavelength. Moreover, the electron transfer upon direct excitation of the perylene bisimide is much faster in the square (2 ps) as compared to the ligand (80 ps). Indeed, 2 ps is an extremely fast rate for an electron-transfer process if we consider the

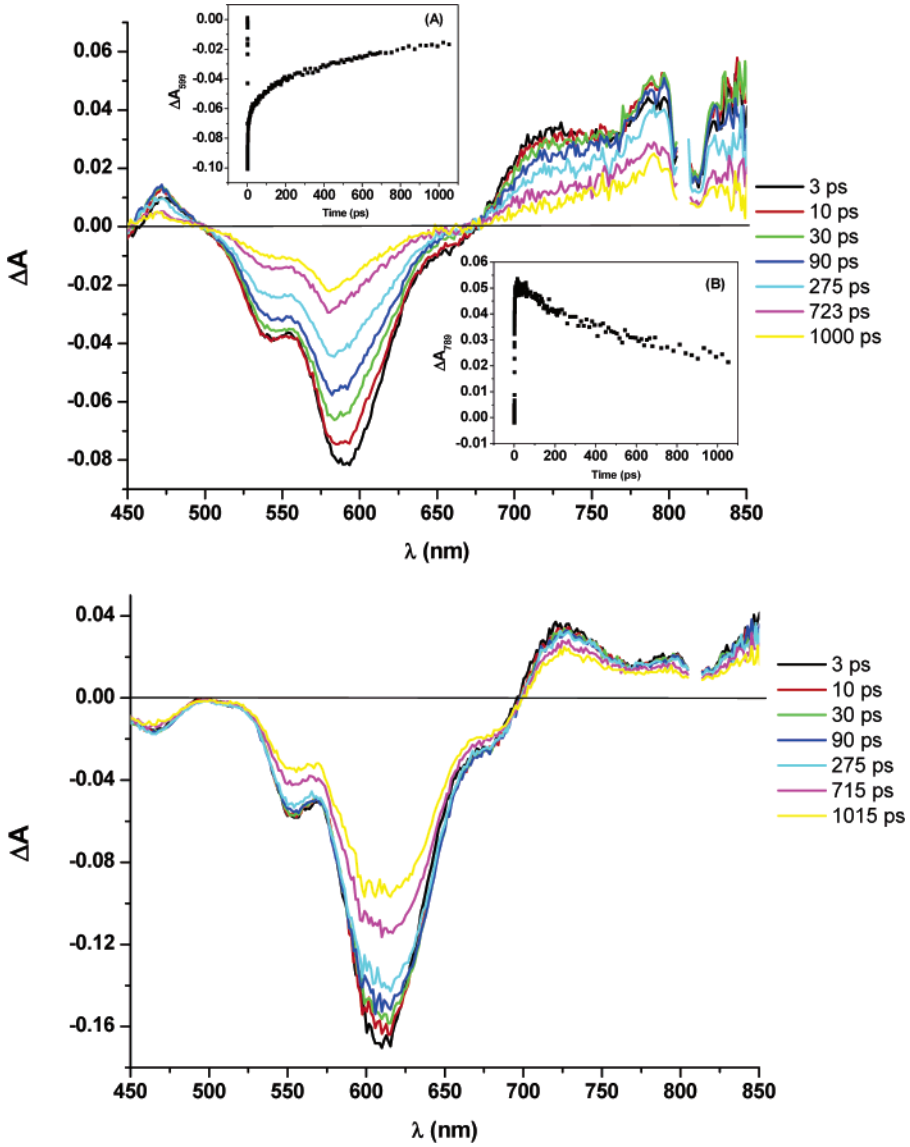

Figure 8. Femtosecond transient spectra of **Sq1** (top) and **Sq2** (bottom) in dichloromethane; time delays corresponding to frames are given in the spectra (λ_{ex} = 575 nm, 130 fs fwhm). Kinetic profiles of the transient absorbance of **Sq1** measured at 599 nm (A) and 789 nm (B) in dichloromethane.

significant distance between the pyrene and the perylene bisimide chromophores in Figure 3.

Spectrotemporal Parametrization. The kinetic profiles for the electron-transfer processes are difficult to analyze by single wavelength fitting because both energy- and electron-transfer reactions take place after 345 nm excitation. For this reason, the femtosecond transient absorption data-matrices in conjunction with the single photon counting data of **Sq1** and **L1** were analyzed with spectrotemporal parametrization, an advanced global and target analysis method[34] also used for complex biological systems such as photosystems. This analysis gives a more in-depth view of the processes that occur in the light-harvesting square (see Scheme 2) because the time information at every wavelength is analyzed, and a target analysis is applied. Not only does this analysis indicate chromophoric heterogeneity (denoted by, e.g., Per*, 'Per*, etc. in Scheme 2), it also shows very fast upper excited-state processes from the first and second excited singlet state of the pyrene (1Py* and 2Py*) to the charge transfer state (CT), as well as branching. Furthermore, it allows a better evaluation of the effects of supramolecular organization by comparing **Sq1** and **L1**.

In the case of visible excitation (575 nm) into the S_1 state of perylene bisimide, the global fit resulted in four rates of charge separation: 0.12, 2.1 (major component), 90, and 800 ps. Furthermore, a very fast (0.12 ps) solvation process is observable. Charge recombination occurs with a time constant of ca. 0.6 ns. The origin of four kinetic components of the charge-transfer process can be the more facile oxidation of some pyrene groups in **Sq1**, as observed in the case of ferrocene-functionalized perylene bisimide squares in electrochemical experiments.[5b] According to X-ray analysis and molecular modeling, substitution at the bay area of perylene bisimides leads to a twist of the two naphthaleneimide units by ca. 30°.[35,36] This twisting of the

(34) (a) van Stokkum, I. H. M.; Larsen, D. S.; van Grondelle, R. *Biochim. Biophys. Acta* **2004**, *1657*, 82−104. (b) van Stokkum, I. H. M.; Lozier, R. H. *J. Phys. Chem. B* **2002**, *106*, 3477−3485. (c) The full analysis of the square and ligand: manuscript in preparation.

(35) Würthner, F.; Sautter, A.; Thalacker, C. *Angew. Chem., Int. Ed.* **2000**, *39*, 1243−1245.

(36) Hofkens, J.; Vosch, T.; Maus, M.; Köhn, F.; Cotlet, M.; Weil, T.; Herrmann, A.; Müllen, K.; De Schryver, F. C. *Chem. Phys. Lett.* **2001**, *333*, 255−263.

Scheme 2. Energy Level Diagrams of **Sq1** in Dichloromethane Showing Energy and Electron-Transfer Pathways Obtained with Global and Target Analysis, together with the Main Decay Times Corresponding to the States[a]

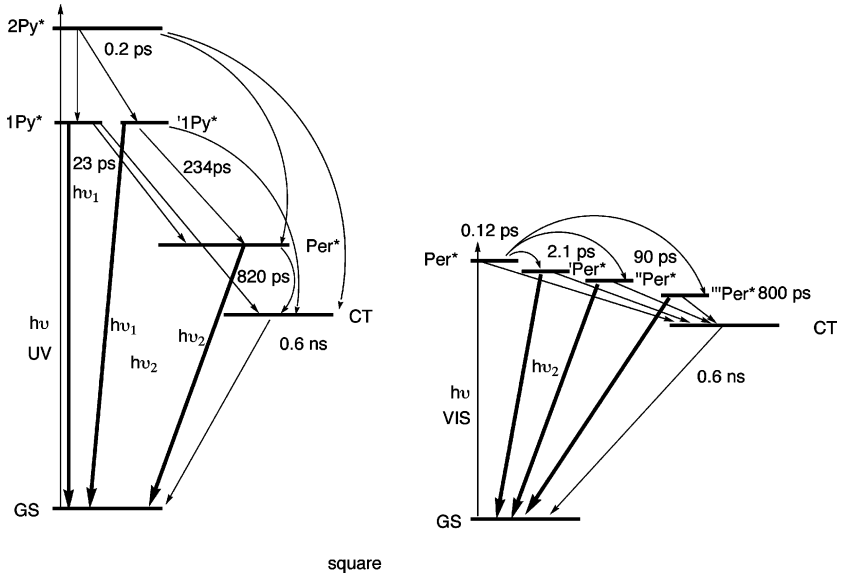

[a] Left: Excitation of pyrene units. Right: Excitation of perylene bisimide units. Bold arrows are radiative processes. Chromophoric heterogeneity is indicated (by, e.g., Per*, 'Per*). Indicated are the first (1Py*) and second (2Py*) excited singlet states of pyrene, the first excited state of the perylene bisimide (Per*), the charge transfer state (CT), and the ground state (GS).

aromatic plane effects the conformations of the appended pyrene (or ferrocene in ref 5b) units by separating them into two groups: one set is pointing toward the inside of the square cavity, while the other set orients toward the outside (cp. Figure 3A). Thus, the different electron-transfer rates can be attributed to different processes involving either the inside or the outside pyrene units of the supramolecular square.

The results obtained upon UV excitation (345 nm) in the S_2 state of pyrene show a very complex cascade-like process with different energy and electron-transfer pathways. An ultrafast component (0.2 ps) corresponds to the decay of the $S_2 \rightarrow S_1$ state of the pyrene, as well as to a small amount of growth (10%) of the charge separated state. This indicates upper excited-state electron transfer. Also from the S_1 state of pyrene charge separation occurs with a 23 ps time constant. The 234 ps component is common for the energy and electron-transfer processes. Note the excellent agreement with the time-resolved emission data. The 0.6 ns component is ascribed to the decay of the charge-separated state.

The processes occurring upon excitation of **Sq1** with either visible or UV light are depicted in the energy diagram in Scheme 2, which also shows that chromophoric heterogeneity is observed for Per* and 1Py*. For the ground (GS), 2Py*, and CT states, no spectral or temporal proof is available for the presence of different kinds of states. Furthermore, two energy transfer pathways are available from the first excited singlet states of the (two different) pyrenes. The main decay times are denoted in Scheme 2, close to the decaying states. Whereas this refined picture appears very complex, the major (70−90%) processes are as described in the previous sections. It has to be noted that analysis of the single line kinetics gives slightly different time constants due to the fact that for the global analysis all wavelengths and, thus, all data are taken into account. The time constants obtained in the global analysis are considered to be more accurate.

Interestingly, the analysis does not provide evidence for an equilibrium between the charge transfer state and the perylene excited state. Such a process was observed recently in triphenylamine-perylene bisimide dendrimers by single molecule spectroscopy by De Schryver and co-workers[18e] and considered also as a possibility for the pyrene-perylene bisimide chromophore pair in our earlier study with the ligand.[21] However, our current study clearly shows that such an equilibrium is not present in **Sq1** and **L1**, as no indication for it is found in the spectro-temporal analysis. There is no sign for equilibrium in the decay associated difference spectra. This argument can also be understood by the difference in the transient absorption spectra obtained with UV or visible excitation at, for example, 275 ps (see Figures 7 and 8, e.g., ratio 720 and 780 nm bands), because after the energy transfer from ^{1}Py* is completed, the same equilibrium would be reached by UV or vis excitation if electron transfer is fast.

Comparison of the data obtained for **Sq1** and **L1** shows that upon UV excitation (345 nm) the spectral features are very similar. However, the rates obtained for the square are slightly higher. This difference is larger for visible excitation, where the major rates obtained for the square are more than 1 order of magnitude higher. Also, the yields of charge separation and energy transfer are substantially higher for the square. Close inspection of the data of **Sq1** also indicates that the yield of charge separation is larger for UV excitation of the square than for visible excitation.

In general, the analysis[34c] shows that the molecular square is not only structurally very complex, but also its excited-state processes appear to become as complex as that observed in, for example, natural photosystems.

As an example, the species associated difference spectra and their time profiles are given in Figure 9. In this analysis, the chromophoric heterogeneity of the first excited singlet state of pyrene is observed (black and green spectrum). The 1Py* spectrum obtained from the analysis of the ligand (black spectrum) was used as a model for the "outside" pyrene units, and an excellent fit resulted in a blue-shifted spectrum of '1Py* (green). This state decays slower than 1Py*, implying a different

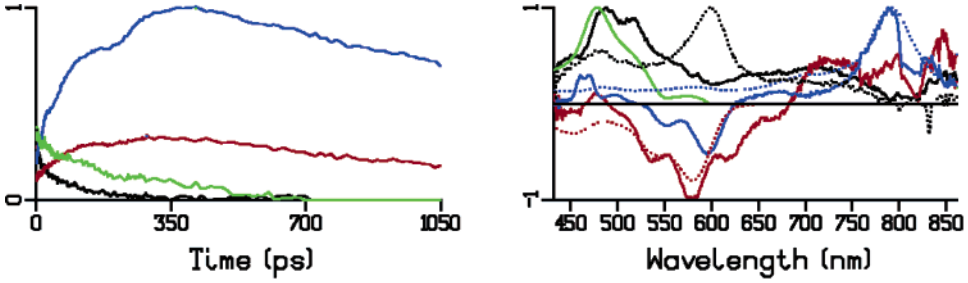

Figure 9. Right: Normalized species associated difference spectra obtained with spectrotemporal analysis. Shown are: black, first excited singlet state of the pyrene (1Py*); green, '1Py* (chromophoric heterogeneity); blue, charge transfer state; red, excited-state absorption and emission of the perylene bisimide. Dotted black: 2Py* state. For comparison, the radical anion spectrum obtained for **Sq2** obtained with spectroelectrochemistry (dotted blue) and the (negative) UV−vis absorption spectrum of **Sq2** (dotted red) are also shown. Left: Concentration profiles versus time of the four species described above in the same colors.

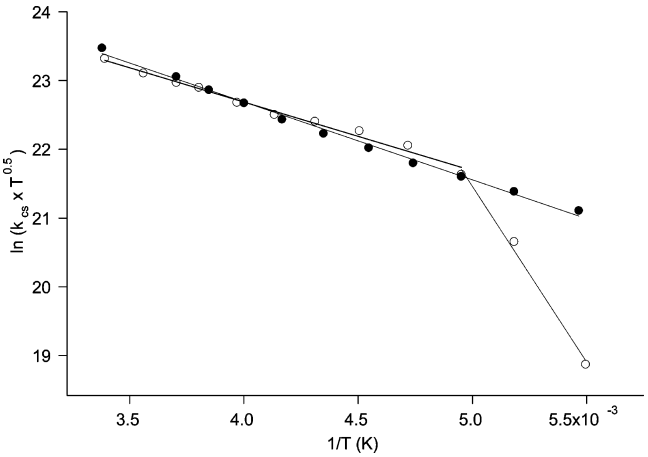

Figure 10. Modified Arrhenius plot for photoinduced charge separation of **Sq1** (●) and **L1** (○) in dichloromethane (λ_{ex} = 324 nm), referring to the major emission component.

coupling with the perylene bisimide. The spectrum denoted in blue shows the pure charge transfer state, and the agreement in the 700−850 nm region with the spectro-electrochemically created radical anion spectrum (dotted blue) is obvious. Also the excited-state absorption of the perylene bisimide is in good agreement with the transient absorption spectrum of the reference **Sq2** (Figures 7 and 8).

Inspection of the time profiles indicates that the pyrene chromophores denoted by the black curve contribute more to the electron-transfer processes (than the ones denoted by the green curve), as it corresponds better to the fast rise of the blue curve. The time-profile of 2Py* is not shown, but this state is responsible for the ultrafast formation of the CT state; therefore, the blue curve does not start at zero. Thus, the four rates of charge transfer state formation from four different states are exemplified by the concentration profiles of these species.

Temperature-Dependent Time-Resolved Emission Spectroscopy. To deduce the barrier for the photoinduced electron-transfer process, as determined previously for **L1**,[21] the excited-state lifetimes of **Sq1** were measured at temperatures in the range between 296 and 183 K and were analyzed using a modified Arrhenius plot (see Figure 10). From the slope of $\ln(k_{cs} \times T^{0.5})$ versus $1/T$, the value of $\Delta G^{\#}$ can be estimated.[37] For this analysis, the major longer living component of **Sq1** was used. The room-temperature lifetime of the **Sq2** was used as a reference in dichloromethane (5.5 ns). All of the data of **Sq1** and of **L1** are summarized in Table 2, in which τ is the lifetime

Table 2. Acceptor Emission Decay Time at 615 nm in Dichloromethane at Various Temperatures, λ_{ex} = 324 nm, Reported for **Sq1** and **L1**[21]

T (K)	τ (ns) [**Sq1**] at 615 nm	T (K)	τ (ns) [**L1**] at 615 nm
296	0.915	295	1.05
		281	1.22
270	1.232	270	1.34
260	1.408	263	1.4
250	1.594	252	1.62
240	1.851	242	1.81
230	2.083	232	1.91
220	2.330	222	2.06
211	2.602	212	2.32
202	2.844	202	2.9
193	3.160	193	4.22
183	3.442	182	5.52

of the perylene emission obtained from the decay at 615 nm after excitation at 324 nm, and k_{cs} is the rate constant calculated according to

$$k_{cs} = 1/\tau - 1/\tau_{ref} \qquad (2)$$

By using the electron-transfer rates from Table 2, the modified Arrhenius plot is constructed. It clearly shows a straight line for the temperature range studied. In contrast to **L1**, only one barrier value ($\Delta G^{\#}$ = 0.098 eV, $\ln(k_{opt})$ = 27.25 [=intercept] for **Sq1**) could be calculated from the slope of this curve (see Figure 10). For the individual ligand **L1**, two barrier values (0.08 and 0.42 eV, $\ln(k_{opt})$ = 26.46 for **L1**) were obtained by fitting two different temperature ranges.[21]

The rise time of the perylene emission is virtually temperature independent for the ligand (**L1**) and the square (**Sq1**) and corresponds to the fast decay of the pyrene emission.

Interestingly, if we compare the data obtained for the ligand (**L1**) and the square (**Sq1**), we can observe a clear difference at the low temperatures. There are two possible explanations for the difference in temperature behavior: the charge separation slows down suddenly for **L1**, but not for **Sq1**, due to a slightly different energetics (larger driving force, and smaller barrier for **Sq1**). The other explanation is that there is a conformational change in the lower temperature range for **L1**, but not for **Sq1**. As the energetics of both systems are almost identical, the latter explanation appears more appealing.

A theoretical approximation of the barrier value can be obtained by using the λ (reorganization energy), ΔG_{cs} (Gibbs

(37) Kroon, J.; Oevering, H.; Verhoeven, J. W.; Warman, J. M.; Oliver, A. M.; Paddon-Row, M. N. *J. Am. Chem. Soc.* **1993**, *115*, 5065−5069.

free energy change for charge separation), and the Marcus model.[38,39] We can estimate the driving force (ΔG_{cs}) from the electrochemical data (E_{ox} = 1.4 V vs SCE and E_{red} = −0.4 V vs SCE),[8] and the singlet state energy (E_{00} = 2.07 eV). The solvent reorganization energy (λ) can be calculated, and an estimate of the internal reorganization is 0.1 eV. The center-to-center distance (R_c) between the two chromophores can be obtained from the 3D model (Figure 3) and is ∼15 Å. An average ionic radius of 6.5 Å is assumed. Thus, using the standard Rehm−Weller approach, in combination with the Marcus model, gives a driving force of −0.09 eV, a total reorganization of 0.58 eV, and a theoretical barrier to electron transfer of 0.1 eV, in good agreement with the experimentally obtained value.

Thus, the different temperature dependence (at the lower temperatures) observed for **Sq1** in dichloromethane (as compared to **L1**)[21] confirms our hypothesis on conformational differences between **Sq1** and **L1**, reported in previous sections. While the pyrene units exhibit significant degrees of freedom in **L1**, they are sterically more confined within **Sq1**. This is an important result as it shows that upon metal-ion directed square formation a more rigid nanostructure is formed that leads to a faster charge separation in the supramolecular system as compared to its precursor ligand. As also in nature such features arise within circular multichromophoric light-harvesting dye assemblies,[40] our observations for artificial self-assembled squares might point at a general phenomenon for such structurally highly confined nanosystems. Nevertheless, it has to be emphasized that in the natural assemblies chromophores are not only rigidified but in addition positioned in a very precise manner in space with the help of proteins, a feature that is not shared by our supramolecular squares.

Conclusions

For the first time, molecular squares have been applied to build up a complex multichromophoric superstructure, which exhibits structural and functional features related to examples found in natural photosynthetic pigments. For this work, perylene bisimide ligands were equipped with pyrene antenna chromophores and subject to transition metal ion-directed self-assembly to yield the molecular square **Sq1** that assembles a total of 16 pyrene antenna dyes and four perylene bisimide dyes in defined spatial orientation. Characterization by multinuclear NMR spectroscopy and ESI-FTICR-MS gives clear proof of the structure and stability of **Sq1**.

The photophysical properties of **Sq1** have been investigated by steady-state and time-resolved spectroscopy. These studies clearly show that the pyrene containing molecular square is a light-harvesting system that combines a fast (k_{en} = 5.0 × 10^9 s^{-1}) and efficient (90%) energy transfer with a very fast and even more efficient (>94%) electron-transfer process with rates of 5 × 10^{11} to 43 × 10^{11} s^{-1} upon visible excitation.

In comparison to the ligand **L1**, there is a large acceleration of the electron transfer in **Sq1** and an increase in efficiency from 70% to >94%. Three reasons have been identified to account for this rate acceleration, which are the lower LUMO level of the perylene bisimide caused by coordination to the metal ion (improved acceptor capability), the rigidification of the system imposed by steric crowding, and the increase in local concentration of chromophores. In this respect, the molecular square composed of 20 chromophores that are closely packed in a small volume might be considered as an interfacial structure that approaches the solid state. Indeed, the extremely fast electron-transfer rates corresponding to the 2.1 and 0.2 ps components observed in the global analysis (5 × 10^{11} and 43 × 10^{11} s^{-1}) are in the range of processes such as charge injection in nanocrystalline TiO_2 in dye sensitized solar cells[41] and photoisomerization of rhodopsin in vision.[42] These surprising results indicate that we might also consider these molecular squares as monodisperse nanoaggregates, a molecularly defined ensemble of chromophores that partly behaves like a solid material.

Acknowledgment. This work was supported by the Volkswagen Foundation within the framework program "Physics, Chemistry and Biology with single molecules". Financial support from the DPI (Dutch Polymer Institute) for M.Z., from NWO (Nederlandse organisatie voor Wetenschappelijk Onderzoek) for the femtosecond equipment, and from the UvA (Universiteit van Amsterdam) for B.K.K., L.D.C., and R.M.W. is gratefully acknowledged. We would like to thank the referees of this paper for their valuable suggestions, which were helpful in improving the work significantly.

Supporting Information Available: Experimental section and a description of the spectroscopic equipment. This material is available free of charge via the Internet at http://pubs.acs.org.

JA0448216

(38) Marcus, R. A. *J. Chem. Phys.* **1956**, *24*, 966−978.
(39) Marcus, R. A.; Sutin, N. *Biochim. Biophys. Acta* **1985**, *811*, 265−322.
(40) (a) Pullerits, T.; Sundström, V. *Acc. Chem. Res.* **1996**, *29*, 381−389. (b) Hu, X.; Schulten, K. *Phys. Today* **1997**, *50*, 28−38.
(41) (a) O'Regan, B.; Graetzel, M. *Nature* **1991**, *353*, 737−739. (b) Tachibana, Y.; Moser, J. E.; Graetzel, M.; Klug, D. R.; Durrant, J. R. *J. Phys. Chem.* **1996**, *100*, 20056−20062. (c) Asbury, J. B.; Ellingson, R. J.; Ghosh, H. N.; Ferrere, S.; Nozik, A. J.; Lian, T. Q. *J. Phys. Chem. B* **1999**, *103*, 3110−3119.
(42) (a) Hoff, W. D.; Jung, K. H.; Spudich, J. L. *Annu. Rev. Biophys. Biomol. Struct.* **1997**, *26*, 223−258. (b) Schoenlein, R. W.; Peteanu, L. A.; Mathies, R. A.; Shank, C. V. *Science* **1991**, *254*, 412−415. (c) Mathies, R. A.; Lin, S. W.; Ames, J. B.; Pollard, W. T. *Annu. Rev. Biophys. Biophys. Chem.* **1991**, *20*, 491−518.